Polish Society of Composite Materials
Polskie Towarzystwo Materiałów Kompozytowych

13: 2 (2013) 122-127

COMPOSITES THEORY AND PRACTICE

Roman Gieleta, Paweł Gotowicki*, Arkadiusz Popławski

Military University of Technology, Department of Mechanics and Applied Computer Science, ul. gen. S. Kaliskiego 2, 00-908 Warsaw, Poland
** Corresponding author. E-mail: pgotowicki@wat.edu.pl*

Received (Otrzymano) 15.02.2013

STRAIN RATE EFFECTS ON SELECTED MECHANICAL PROPERTIES OF GLASS-POLYESTER LAMINATES

The study presents the results of experimental testing of a layered cross-ply $[0/90]_n$ E-glass/polyester composite in the range of the selected compression properties at high strain rates = 2300÷4600 s^{-1} and a quasi-static strain rate = 0.0067 s^{-1}. The composite was manufactured using contact technology using Owens Corning CD-600 E-glass stitched fabric and Polimal 104 polyester resin. The circular cross-section specimens of three sizes 2.5, 5 and 7.5 mm in height and 15 mm in diameter were tested in the above described experiments. To determine the static properties, quasi-static experimental tests were conducted using an Instron 8802 machine in the displacement control mode at a constant crosshead speed of 1, 2 and 3 mm/min respectively for the 2.5, 5.0 and 7.5 mm specimen types. The compression loading was monitored with a load cell Instron ±250 kN, whereas the axial strain with an Instron 2620-604 extensometer using additional fixing discs. The measuring base of the extensometer was equal to the specimen height. Identification included the stress-strain curve, strength, Young's modulus and failure strain. For the high strain rates testing, a modified Split Hopkinson Pressure Bar test system was used, containing an LTT 500 Amplifier made by Tasler, Germany and an NI USB-6366 data acquisition device made by National Instruments, USA. The failure modes observed under high strain rate loading were similar to those observed under quasi static loading. The samples predominantly failed by shear fracture. Reduction of the specimen height implies an increase in the nonlinear effects in the initial part of the stress-strain diagrams (increasing strain at same stress), probably caused by the boundary effect. The main parts of the stress-strain plots are approximately linear, thus the linear elastic-brittle material model can be assumed. It was generally observed that the compressive strength and Young's modulus along the thickness direction are higher at high strain rate loading compared to the results at quasi-static loading.

Keywords: layered composite, glass-polyester composite, high strain rate, SHPB

WPŁYW PRĘDKOŚCI ODKSZTAŁCEŃ NA WYBRANE WŁAŚCIWOŚCI MECHANICZNE LAMINATU POLIESTROWO-SZKLANEGO

W pracy przedstawiono wyniki badań eksperymentalnych laminatu krzyżowego $[0/90]_n$ szkło-E/poliester w zakresie wyznaczenia właściwości mechanicznych podczas ściskania z prędkością =2300÷4600 s^{-1} w badaniach dynamicznych oraz = 0,0067 s^{-1} w badaniach quasi-statycznych. Badany kompozyt wytworzono metodą kontaktową z użyciem tkaniny zszywanej Owens Corning CD-600 oraz żywicy poliestrowej Polimal 104. Do badań przyjęto trzy typy próbek walcowych o wysokości 2,5; 5 i 7,5 mm oraz średnicy 15 mm. W celu wyznaczenia właściwości mechanicznych statycznych przeprowadzono badania eksperymentalne z wykorzystaniem maszyny wytrzymałościowej Instron 8802 w trybie sterowania przemieszczeniem, z prędkością przemieszczenia 1, 2 and 3 mm/min, odpowiednio dla próbek typu 2,5, 5,0 i 7,5 mm. Obciążenie rejestrowano przy użyciu głowicy pomiarowej Instron ±250 kN. Pomiar odkształcenia realizowano z użyciem ekstensometru Instron 2620-604 z dodatkowym oprzyrządowaniem w postaci dysków. Baza pomiarowa ekstensometru była równa wysokości próbki. Badania identyfikacyjne obejmowały wyznaczenie zależności naprężenie-odkształcenie, wytrzymałości, modułu sprężystości oraz odkształceń niszczących. Badania przy dużej prędkości odkształceń przeprowadzono na stanowisku Zmodyfikowany Pręt Hopkinsona (SHPB - Split Hopkinson Pressure Bar), stosując wzmacniacz LTT 500 firmy Tasler, Niemcy oraz kartę pomiarową NI USB-6366 firmy National Instruments, USA. Zaobserwowano podobny mechanizm niszczenia próbek w badaniach quasi-statycznych oraz dynamicznych. Próbki niszczyły się przez ścinanie. Zmniejszenie wysokości próbki powoduje ujawnienie się efektów nieliniowych w początkowej części wykresów (zwiększenie odkształcenia przy tym samym naprężeniu). Jest to związane z efektem brzegowym. Środkowa część zależności naprężenie-odkształcenie jest w przybliżeniu liniowa, co odpowiada materiałowi liniowo-sprężysto-kruchemu. W wyniku badań zaobserwowano wzrost wytrzymałości na ściskanie oraz modułu sprężystości w kierunku prostopadłym do powierzchni warstwy laminatu wraz ze wzrostem prędkości odkształceń.

Słowa kluczowe: kompozyty warstwowe, kompozyt poliestrowo szklany, duża prędkość odkształceń, pręt Hopkinsona

INTRODUCTION

Fibre reinforced composites have material properties which are attractive for use in various engineering applications. High specific stiffness and strength under static and especially under dynamic loading conditions

make these materials very useful for military applications. Understanding of material response to dynamic loadings is achieved through experimental and theoretical analyses and requires the development of constitutive equations which could be used to explain the variation in material strength, stress and strain versus strain rates. The most extensively used apparatus for high strain rate material characterization is the Split Hopkinson Pressure Bar (SHPB). The split bar technique for the dynamic testing of materials was introduced by Kolsky [1]. The working rule of the SHPB apparatus is based on the one-dimensional wave propagation theory in elastic bars. To determine the behaviour of composites under high strain rate loading, the SHPB apparatus is used widely. So far, various experimental studies were carried out on the high strain rate behaviour of composites under compressive loading. Available studies on cross-ply composites made of glass fibres were presented in [2-5] and on carbon fibres in [6-9]. Information about the properties at high strain rates compared to those at the quasi-static strain rate and the property change factor is given in Table 1. Glass and carbon materials, resin and fibre volume fractions are different for particular studies. The property change factor is generally more than one for compressive strength and Young's modulus. The property change factor varies in a wide interval in the analysed contributions. Note that the property change factor is defined as the ratio of the property at high strain rate (HSR) loading to the property at low strain rate (LSR) loading.

EXPERIMENTAL PROCEDURES

This study concerns the glass polyester cross-ply laminate, i.e. Polimal 104 polyester resin reinforced with CD-600 E-glass non-woven fabric made by Owens Corning, USA (Biaxial, orthogonal [0/90], 610 g/m^2, stitched 283/317/10 tex). The composites and specimens were manufactured in the Department of Mechanics and Applied Computer Science, at the Military University of Technology. Figure 1 presents the principal directions of the laminate. The prefabricated elements used to manufacture the specimens for compression tests were cut using water jet technology according the scheme in Figure 2. After the cutting process, the specimens were lathed to obtain nominal diameter d = 15 mm.

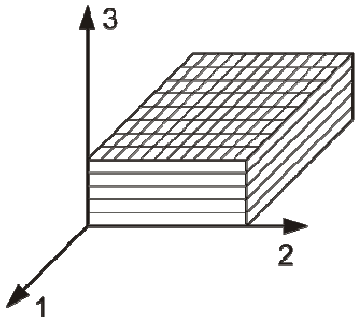

Fig. 1. Principal directions of laminate (1-2 - laminate plane; 3 - thickness direction)

Rys. 1. Kierunki wzmocnienia laminatu (1-2 - płaszczyzna laminatu; 3 - kierunek grubości)

TABLE 1. **Mechanical properties and property change factor of composites under compressive loading; 1 - warp direction, 2 - weft direction, 3 - thickness direction [10]**

TABELA 1. **Właściwości mechaniczne oraz współczynnik zmiany właściwości dla kompozytu w próbie ściskania; 1 - kierunek osnowy, 2 - kierunek wątku, 3 - kierunek grubości [10]**

Composite	Dir.	strain rate [s^{-1}]	LSR properties			Property change factor HSR/LSR			Ref.
			σ^{ult} [MPa]	E [GPa]	ε^{ult} [%]	σ	E	ε	
plain weave S2-glass/vinylester	2	1149	180	5.00	3.60	1.75	3.30	0.61	[2]
plain weave glass/epoxy	1	860	410	20.8	2.23	1.40	1.39	1.26	[3]
plain weave S2-glass/vinylester	2 3	705 675	292 690	- -	1.20 5.20	1.41 1.35	- -	2.21 1.36	[4]
woven S2-glass	1 3	840 800	265 600	- -	2.40 4.55	1.92 1.16	- -	1.13 1.57	[5]
woven carbon/epoxy	2	600	507	-	0.93	1.80	-	1.83	[6]
plain weave carbon/epoxy	1	1039	196	8.3	3.90	2.27	4.24	0.38	[7]
satin weave carbon/epoxy	1 2	1092 1079	227 237	11.1 11.7	3.40 3.00	2.31 2.36	4.05 3.90	0.44 0.53	[7]
plain weave graphite/epoxy	1	930	196	8.3	3.90	2.50	4.90	0.38	[8]
satin weave graphite/epoxy	1 2	945 977	227 237	11.0 11.0	3.40 3.00	2.40 2.43	3.90 3.90	0.51 0.54	[8]
satin weave carbon/epoxy	1 2	1092 1390	312 358	4,70 4,87	9.4 10.7	1.33 1.46	4.63 5.62	0.27 0.23	[9]

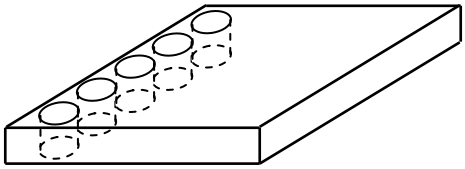

Fig. 2. Prefabricated elements for compression specimens manufacturing process scheme

Rys. 2. Sposób przygotowania półfabrykatów do wykonania próbek na ściskanie

For the study aims, three types of specimens were used, indicated with symbols reflecting the specimen height, i.e. 7.5, 5.0 and 2.5 - Figure 3.

Fig. 3. Specimens before testing

Rys. 3. Widok próbek przed próbą

In the static experimental study, the specimens were subjected to uniaxial compressive loading with a constant crosshead speed of 1, 2 and 3 mm/min for 2.5, 5.0 and 7.5 specimen types, respectively, with the same strain rate for all specimens i.e. = 0.0067. The experiments were conducted using a servohydraulic, universal testing machine, Instron 8802. The compression loading was monitored with the load cell, whereas the axial strain with an Instron 2620-604 extensometer using additional fixing discs. The measuring base was equal to the sample height. The circular cross-section specimens of three sizes were tested in the above described experiments. Identification included the stress-strain curve, strength, Young's modulus and failure strain.

For high strain rates testing, a modified Split Hopkinson Pressure Bar test system was used (Fig. 4), containing an LTT 500 Amplifier made by Tasler, Germany and an NI USB-6366 data acquisition device made by National Instruments, USA.

Basically, the test system consists of a gas gun, a striker (20 mm diameter, 150 mm long), an incident bar, a transmission bar (both 20 mm diameter and 2000 mm long), an energy absorption element and a data acquisition system. The striker is launched using highly compressed gas and impacts the incident bar. This generates the elastic wave (the incident wave) which travels through the bar and then, due to the difference between the mechanical impedance of the bar and specimen materials, part of the pulse comes back (the reflected wave), whereas the residual part is transmitted through the tested specimen. Consequently, it compresses it and the wave travels to the transmission bar and generates the so called transmitted wave. All three signals were registered by the strain gauges which are placed in the middle of the bars, as shown in Figure 5.

Fig. 4. Compressive Split Hopkinson Pressure Bar test system

Rys. 4. Stanowisko Zmodyfikowany Pręt Hopkinsona do pomiarów właściwości wytrzymałościowych materiałów przy ściskaniu

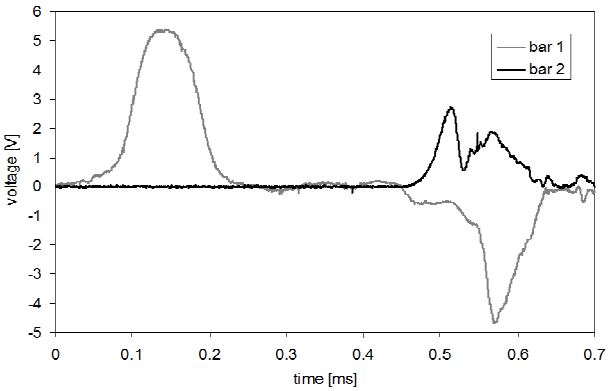

Fig. 5. Signals registered using strain gauges placed in middle of bars

Rys. 5. Sygnały zarejestrowane z wykorzystaniem tensometrów naklejonych w połowie długości prętów

RESULTS

During the static tests, the stresses and strains were calculated using the formulas:

$$\sigma = \frac{F}{A_s} = \frac{4 \cdot F}{\pi \cdot d^2} \tag{1}$$

where:

σ - engineering stress [MPa]
F - force [N]
A_s - cross-section area of specimen [mm^2]
d - specimen diameter [mm]

$$\varepsilon = \frac{\Delta L}{L} \tag{2}$$

where:
ε - engineering strain [-],
L - length of specimen (extensometer measuring base) [mm]
ΔL_0 - length change [mm].

Based on the recorded signals the strains, stresses and strain rates were calculated using formulas [1]:

$$\varepsilon(t) = \frac{\Delta L}{L} - 2\frac{C_o}{L}\int_0^t \varepsilon_R(t)dt \tag{3}$$

$$\sigma(t) = \frac{EA_b}{A_s}\varepsilon_T(t) \tag{4}$$

$$\dot{\varepsilon}(t) = -2\frac{C_o}{L}\varepsilon_R(t) \tag{5}$$

where:
C_o - wave velocity in bars,
E - Young's modulus of bars,
A_b - cross-sectional area of bars,
$\varepsilon_R(t)$ - reflected strain pulse,
$\varepsilon_T(t)$ - transmitted strain pulse,
$\dot{\varepsilon}(t)$ - strain rate in the specimen.

The experimentally obtained compressive stress–strain curves for the laminate along thickness (3) the direction at strain rates up to 4600 s^{-1} are presented in Figures 6-10. The stress-strain plots for the 7.5, 5.0 and 2.5 specimen types with respect to the specimen height, obtained from the static and high strain rate tests, are compared in Figures 6 and 7, respectively.

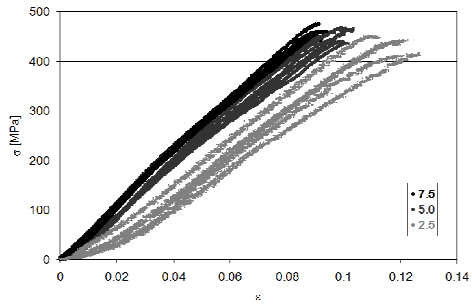

Fig. 6. Static stress-strain response of 7.5, 5.0 and 2.5 specimen types ($\dot{\varepsilon}$ = 0.0067 s^{-1})

Rys. 6. Zależność σ-ε dla próbek typu 7,5, 5,0 i 2,5 przy małych prędkościach odkształceń ($\dot{\varepsilon}$ = 0.0067 s^{-1})

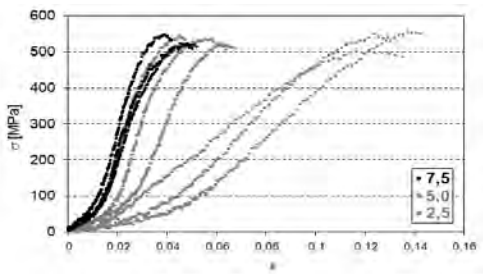

Fig. 7. High strain rates stress-strain response of 2.5, 5.0 and 7.5 specimen types ($\dot{\varepsilon}$ = 4600 s^{-1}, $\dot{\varepsilon}$ = 2400 s^{-1}, $\dot{\varepsilon}$ = 2300 s^{-1})

Rys. 7. Zależność σ-ε dla próbek typu 2,5, 5,0 i 7,5 przy dużych prędkościach odkształceń (odpowiednio $\dot{\varepsilon}$ = 4600 s^{-1}, $\dot{\varepsilon}$ = 2400 s^{-1}, $\dot{\varepsilon}$ = 2300 s^{-1})

The stress-strain plots with respect to the strain rates, obtained for the static and high strain rate tests for the 7.5, 5.0 and 2.5 specimen types are compared in Figures 8, 9 and 10 respectively.

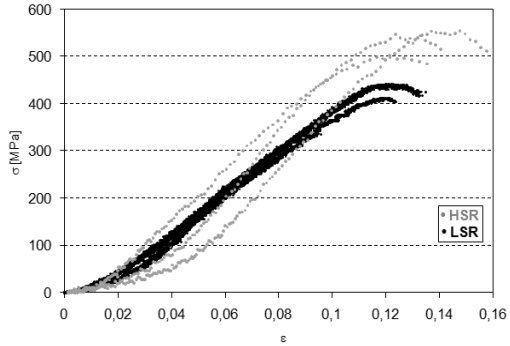

Fig. 8. Stress-strain plots for strain rates $\dot{\varepsilon}$ = 0.0067 s^{-1} and $\dot{\varepsilon}$ = 4600 s^{-1} for 2.5 specimen type

Rys. 8. Zależność σ-ε dla próbek typu 2,5 dla prędkości odkształceń $\dot{\varepsilon}$ = 0.0067 s^{-1} oraz $\dot{\varepsilon}$ = 4600 s^{-1}

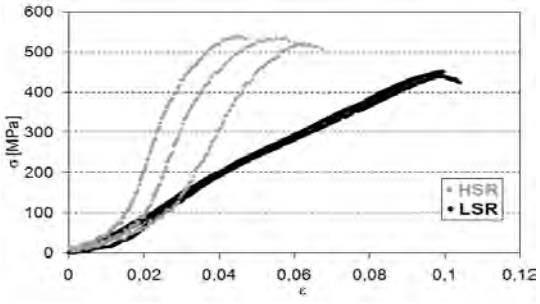

Fig. 9. Stress-strain plots for strain rates and for 5.0 specimen type $\dot{\varepsilon}$ = 0.0067 s^{-1} and $\dot{\varepsilon}$ = 2400 s^{-1}

Rys. 9. Zależność σ-ε dla próbek typu 5,0 dla prędkości odkształceń oraz $\dot{\varepsilon}$ = 0.0067 s^{-1} oraz $\dot{\varepsilon}$ = 2400 s^{-1}

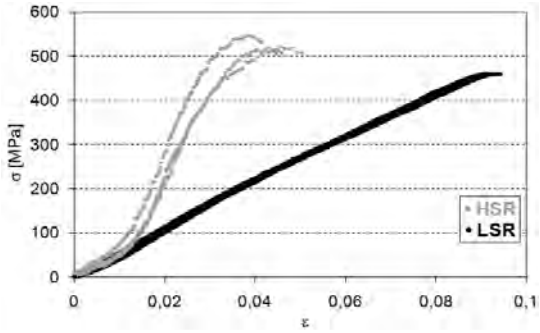

Fig. 10. Stress-strain plots for strain rates $\dot{\varepsilon}$ = 0.0067 s^{-1} and $\dot{\varepsilon}$ = 2300 s^{-1} for 7.5 specimen type

Rys. 10. Zależność σ-ε dla próbek typu 7,5 dla prędkości odkształceń $\dot{\varepsilon}$ = 0.0067 s^{-1} oraz $\dot{\varepsilon}$ = 2300 s^{-1}

Young's modulus E_3 was determined using linear regression due to the measurement fluctuations, based on the interval of the highest tangent.

The mechanical properties at high strain rates compared to those at the quasi-static strain rate, i.e. Young's modulus, compressive strength and failure strain, are collected in Table 2. Failure of the specimen under quasi static loading and under dynamic loading is presented in Figure 11.

TABLE 2. **Dimensions, mechanical properties and property change factor of composite specimens: $\bar{x}$ - mean value, s - standard deviation, [x_1, x_2] - 95% probability confidence interval**

TABELA 2. **Wymiary, właściwości mechaniczne oraz współczynnik zmiany właściwości dla próbek kompozytowych: $\bar{x}$ - wartość średnia, s - odchylenie standardowe, [x_1, x_2] - 95% przedział ufności**

Spec.	Dimension		LSR properties			HSR/LSR		
	h	d	σ^{ult}	E	ε^{ult}	σ	E	ε
	mm	mm	MPa	GPa	m/m			
1	2.55	15.00	411	3.71	0.118			
2	2.54	14.99	440	3.92	0.128			
3	2.54	14.97	442	3.88	0.121			
	-	-	431	3.84	0.122	1.06	1.65	1.24
s	-	-	17	0.11	0.005			
x_1	-	-	388	3.57	0.110			
x_2	-	-	474	4.11	0.135			
1	5.14	14.98	440	5.52	0.099			
2	5.11	14.96	451	6.34	0.099			
3	5.14	14.98	443	5.85	0.097			
	-	-	445	5.90	0.098	1.20	3.85	0.55
s	-	-	6	0.41	0.001			
x_1	-	-	431	4.88	0.095			
x_2	-	-	459	6.93	0.101			
1	7.73	14.96	460	5.54	0.093			
2	7.67	15.00	458	5.94	0.092			
3	7.68	14.99	460	5.46	0.091			
	-	-	459	5.65	0.092	1.15	4.34	0.46
s	-	-	1	0.26	0.001			
x_1	-	-	456	5.00	0.090			
x_2	-	-	462	6.30	0.094			

a)

b)

Rys. 11. Failure of specimens: a) under quasi-static loading b) under dynamic loading

Rys. 11. Próbki zniszczone podczas badań: a) quasi-statycznych b) dynamicznych

CONCLUSIONS

- The experiments were conducted in the strain rate interval range from 0.0067 to 4600 s^{-1} for a typical stitched E-glass fabric/epoxy laminate along the thickness direction under compressive loading.
- Compared to the static properties, the dynamic peak stresses were by 1.06, 1.2, 1.15 times higher. The dynamic modulus was 1.65, 3.85, 4.34 times higher. However, the ultimate strains under dynamic loading was equal to 1.24, 0.55, 0.46 quasi-static ultimate strains for the 2.5, 5.0 and 7.5 specimen types, respectively.
- The failure modes observed under high strain rate loading were similar to those observed under quasi-static loading. The samples predominantly failed by shear fracture.
- Reduction of the specimen height implies an increase in nonlinear effects in the initial part of the stress–strain diagrams (increasing strain at same stress), probably caused by the boundary effect.
- The main parts of the stress-strain plots are approximately linear, thus the linear elastic-brittle material model can be assumed.
- In the quasi-static tests, Young's modulus determined from interval $\varepsilon = 0.04 \div 0.10$, does not depend on the sample height. The strength slightly increases when the specimen height increases. It is probably caused by the boundary effect.

REFERENCES

[1] Kolsky H., An investigation of the mechanical properties of materials at very high rates of loading, Proceedings of the Physical Society 1949, 62, 676-700.

[2] Haque A., Ali M., High strain rate responses and failure analysis in polymer matrix composites - an experimental and finite element study, Journal of Composite Materials 2005, 39, 423-450.

[3] Harding J., Effect of strain rate and specimen geometry on the compressive strength of woven glass-reinforced epoxy laminates, Composites 1993, 24, 323-332.

[4] Gama B.A., Gillespie Jr J.W., Mahfuz H., Raines R.P., Haque A., Jeelani S., et al., High strain-rate behavior of plain-weave S-2 glass/vinyl ester composites, Journal of Composite Materials 2001, 35, 1201-1228.

[5] Song B., Chen W., Weerasooriya T., Quasi-static and dynamic compressive behaviors of a S-2 glass/SC15 composite, Journal of Composite Materials 2003, 37, 1723--1743

[6] Hou J.P., Ruiz C., Measurement of the properties of woven CFRP T300/914 at different strain rates, Composites Science and Technology 2000, 60, 2829-2834.

[7] Hosur M.V., Adya M., Vaidya U.K., Mayer A., Jeelani S., Effect of stitching and weave architecture on the high strain rate compression response of affordable woven carbon/ epoxy composites, Composite Structures 2003, 59, 507-523.

[8] Hosur M.V., Adya M., Jeelani S., Vaidya U.K., Dutta P.K., Experimental studies on the high strain rate compression response of woven graphite/epoxy composites at room and elevated temperatures, Journal of Reinforced Plastics and Composites 2004, 23, 491-514.

[9] Hosur M.V., Alexander J., Vaidya U.K., Jeelani S., Mayer A., Studies on the off-axis high strain rate compression loading of satin weave carbon/epoxy composites, Composite Structures 2004, 63, 75-85.

[10] Ravikumar G., Pothnis J. R., Joshi M., Akella K., Kumar S., Naik N.K., Analytical and experimental studies on mechanical behavior of composites under high strain rate compressive loading, Materials and Design 2013, 44, 246-255.

